



Mesoporous silica–alumina modified by acid leaching as support of Pt catalysts in HDS of model compounds

Zdeněk Vít^{a,*}, Daniela Gulková^a, Luděk Kaluža^a, Snejana Bakardieva^b, Marta Boaro^c

^a Institute of Chemical Process Fundamentals of the ASCR, v.v.i., Rozvojová 135, 165 02 Prague, Czech Republic

^b Institute of Inorganic Chemistry of the ASCR, v.v.i., Husinec-Řež 1001, 250 68 Řež, Czech Republic

^c Dipartimento di Scienze e Tecnologie Chimiche, Università di Udine, I-33100 Udine, Italy

ARTICLE INFO

Article history:

Received 14 June 2010

Received in revised form 18 August 2010

Accepted 23 August 2010

Available online 20 September 2010

Keywords:

Hydrodesulfurization

Mesoporous silica–alumina

Acid leaching

Platinum

ABSTRACT

The potential of mesoporous silica–alumina (MSA) modified by acid leaching as alternative support for Pt catalysts was studied in hydrodesulfurization (HDS) of thiophene and benzothiophene. The supports were characterized by N_2 adsorption, XRD, ^{27}Al MAS NMR, electron microscopy (SEM, HRTEM) and by activities in cyclohexene isomerization and cumene cracking. The composition of the catalysts and Pt dispersion were determined by ICP and H_2 or CO sorption, respectively. Progressive leaching of the parent MSA from 50% Al_2O_3 to 11% Al_2O_3 content led to increase of the BET surface area and exposition of strong acidity. This positively affected the activities of the reduced Pt catalysts in thiophene HDS. Deposition of 1.5 wt.% Pt on MSA (11% Al_2O_3) by using $Pt(NH_3)_4(OH)_2$ as precursor gave the best catalyst, several times more active in thiophene HDS than the weight equivalents of sulfided CoMo/ Al_2O_3 or reduced Pt/HY zeolite. In benzothiophene reaction, its activity was slightly above that of CoMo/ Al_2O_3 and about twofold compared to Pt/HY.

© 2010 Elsevier B.V. All rights reserved.

1. Introduction

Decreasing allowable limits of sulfur content in liquid fuels and treatment of heavier petroleum feedstocks urge to search of the more efficient catalysts for hydrodesulfurization (HDS). Active phases based on noble metals are often considered for some applications as partial alternative to the traditional CoMo (NiMo) formulations. Platinum had been studied from this point of view for both HDS and aromatics hydrogenation. Frequently used supports were amorphous silica–aluminas (ASA) and zeolites. Navarro et al. [1] studied the activity of the ASA and HY zeolite supported Pt catalysts in HDS of dibenzothiophene (DBT) and diesel oil. The activity of sulfided Pt/ASA (0.95% Pt) was little higher than that of CoMo/ Al_2O_3 in HDS of DBT at 320 °C and 3 MPa, while the activity of Pt/HY (1% Pt) was substantially lower. However, in HDS of diesel oil the Pt/HY catalyst was little more active than Pt/ASA and CoMo/ Al_2O_3 . An excellent hydrogenation activity of Pt catalysts is beneficial as well in the deep HDS, where the saturation of aromatic ring facilitates the C–S bond cleavage of the refractory sulfur compounds. From this point of view, the Pt/ASA catalysts have been studied as an alternative to conventional CoMo (NiMo) catalysts for the second stage of the deep HDS. In these studies, the sulfided

Pt/ASA (0.8% Pt) was slightly more active than CoMo/ Al_2O_3 in HDS of DBT, but several times more active in HDS of 4-methyl-DBT and 4-ethyl, 6-methyl-DBT [2,3]. In comparison to alumina, acidic supports are beneficial from several reasons. It is widely accepted that the acidity of supports increases the electron-deficient character of the reduced Pt particles, which leads to higher sulfur tolerance and activity of the reduced Pt catalysts. Niquille-Röthlisberger and Prins [4] showed that activities of the reduced Pt/ASA catalysts in HDS of 4,6-DMDBT at 300 °C and 5 MPa were substantially higher than activity of Pt/ Al_2O_3 . In another study, the rate of tetralin hydrogenation over the reduced Pt catalysts prepared from Al_2O_3 and ASA of different composition increased parallel with the higher support acidities, i.e. from Al_2O_3 to ASA containing 5% Al_2O_3 [5]. Moreover, Sugioka et al. [6] proposed that Brønsted acid sites of acidic supports like ZSM-5 take part with Pt metal sites in thiophene HDS over the reduced Pt/ZSM-5 catalysts.

Discovery of new mesoporous materials of unique properties such as FSM-16, MCM-41 and SBA-15 has stimulated studies with their use as catalyst supports for hydrotreatment. HDS of thiophene has been studied over catalysts prepared by deposition up to 5% Pt. The loading of 2.5 wt.% Pt deposited on FSM-16 gave the catalyst, that in reduced state was comparable to weight equivalent of sulfided CoMo/alumina in thiophene HDS at 350 °C and 0.1 MPa [7]. These highly siliceous solids are generally less acidic than ASA, and thus their properties have often been modified. In other cases, MCM-41 [8] and SBA-15 [9] were modified by incorporation of aluminum, which enhanced their acidities and consequently led to

* Corresponding author. Tel.: +420 220 390 284; fax: +420 220 920 661.

E-mail address: vit@icfp.cas.cz (Z. Vít).

higher HDS activities. Interpolation of the activity data revealed that Pt loading close to 2 wt.% on Al-SBA-15 was as active as CoMo/alumina (Nippon Cyanamid Co.) in thiophene HDS at 350 °C and 0.1 MPa.

A mesoporous silica–alumina (MSA) with BET surface area of 491 m²/g, narrow pore-size distribution ($d_{\text{mean}} = 3.5$ nm) and disordered pore structure has recently been synthesized by cogelification from simple inorganic salts in our laboratory [10]. At first it was studied as a support of Mo catalysts modified by noble metals [11]. It was later found that the Pt/MSA sulfide catalysts showed a fairly good HDS activity during simultaneous HDS of thiophene and HDN of pyridine [12]. We thus attempted to optimize HDS activity of these catalysts by suitable modification of MSA. Its bulk composition corresponds to 50 wt.% Al₂O₃, from which only part can be incorporated into the SiO₄ matrix. This amount can approach around 40%, while the additional part of Al₂O₃ remains free [13]. It was speculated that the free non-acidic Al₂O₃ in MSA restrains the accessibility of the strong acid sites of silica–alumina phase as such and that their gentle unblocking could lead to acidity enhancement. A similar problem is faced when the extra-framework aluminum (EFAL) from USY zeolites and mordenites is removed to improve their catalytic properties. This can be effected by leaching with different agents such as (NH₄)₂SiF₆, Na₂H₂EDTA and HNO₃ [14], HCl [15,16 and references therein] or H₂SO₄ [17,18]. Such treatments had several positive aspects like increased pore volume, surface area, catalytic activity and the amount of exposed acid sites. In the case of mesoporous MCM-41, the extraction by diluted HNO₃ was performed in order to diminish the sodium content. Partial removal of sodium generated strong acidity, increased the surface area and led to the higher activity of NiMo/MCM-41 catalyst in HDS of DBT [19].

The aim of the present work was to evaluate HDS activity which can be achieved with the Pt catalysts prepared from the leached MSA and to ascertain its potential as an alternative catalyst support for HDS. For this purpose, HNO₃ has been chosen as the most appropriate leaching agent because it does not leave undesirable residue after calcination. Activities in cyclohexene isomerization and cumene cracking were used to determine the acidities of the supports leached to different levels. H₂PtCl₆, Pt(NH₃)₄Cl₂ and Pt(NH₃)₄(OH)₂ were selected for deposition of Pt and the activity of the reduced Pt catalysts was evaluated in HDS of thiophene and benzothiophene. The Pt/MSA catalysts were compared with Pt/HY zeolite and industrial CoMo/alumina catalysts.

2. Experimental

2.1. Preparation of supports and catalysts

The parent mesoporous silica–alumina support was synthesized from aqueous solutions of sodium metasilicate and aluminum nitrate without use of pore regulating agents as described in detail elsewhere [10]. The contents of Al₂O₃ and sodium were 50 and 0.18 wt.%, respectively. This sample is termed as MSA50 in the present work. A series of samples with the reduced Al₂O₃ content was prepared by leaching MSA50 (0.16–0.315 mm fraction) with 1 N solution of HNO₃ in a rotary evaporator at 75 °C for 2 h. The amount of HNO₃ was exactly adjusted in order to obtain the samples with desired degree of Al₂O₃ extraction. The products (1–15 g) were washed with distilled water, dried and calcined in a stream of air at 400 °C for 2 h. These solids were denoted by symbols MS_xY_y, where xy stand for Al₂O₃ content in wt.%. Two ion-exchanged samples were prepared from MSA50 in order to reduce the sodium content. This ion-exchange was performed with 3 M aqueous solution of ammonium nitrate (AN) at 20 °C. One sample was exchanged for 4 h and the other two times, always for 20 h with the fresh AN

solution. Both samples were washed, dried and converted to the acidic form by calcination at 400 °C for 2 h.

An Y zeolite in ammonium powder form (Alfa Aesar) with Si/Al ratio = 5 and containing 1.9 wt.% Na was used for preparation of an additional support. First, the residual sodium was exchanged for ammonium by double ion-exchange with 10 M aqueous AN solution at 20 °C for 4 h. Then the dried powder was converted to the H form by its calcination at 500 °C for 6 h in a stream of air, until the evolution of ammonia has stopped. The BET surface area was 580 m²/g and the surface of mesopores 41 m²/g. The powder was pelletized under 2 MPa pressure, crushed and sieved to the fraction of 0.16–0.315 mm, used further as support. The BET area of this fraction was 216 m²/g and the surface of mesopores 26 m²/g.

The Pt catalysts were prepared by impregnation of the selected supports by aqueous solutions of H₂PtCl₆, Pt(NH₃)₄Cl₂ and Pt(NH₃)₄(OH)₂ (all Sigma–Aldrich) in a rotary evaporator at room temperature for 1 h. The Y zeolite was contacted with the solution for 20 h in attempt to achieve homogeneous adsorption. The slurries were evaporated to dryness at 60 °C under vacuum. The amount of the precursor was chosen according to the required Pt loading and the volume of solutions was usually 6–9 ml per g of support. In the case of H₂PtCl₆, pH of the slurry was 3. The pH of the Pt(NH₃)₄Cl₂ solution was adjusted to 9–10 with NH₄OH. The dried catalysts were reduced in H₂ stream at 400 °C (ramp 4 °C/min and 1 h dwell at 400 °C). This temperature was chosen in order to be sure that the Pt complexes were completely reduced and ammonia released from acidic sites of supports. The catalysts were denoted by symbols like 0.92PtN-34, in sequence: the Pt content in wt.%, Pt precursor, and the support (either the percentage of alumina in the MSA or HY for zeolite). The symbols PtC, PtN and PtO stand for H₂PtCl₆, Pt(NH₃)₄Cl₂ and Pt(NH₃)₄(OH)₂, respectively. Industrial CoMo/Al₂O₃ catalyst (S 344, 2.4 wt.% Co, 9.2 wt.% Mo) was sulfided with 10% H₂S in H₂ at 400 °C for 2 h before reactions.

2.2. Characterization of supports and catalysts

The contents of aluminum and sodium in the supports and Pt in the catalysts were determined by inductively coupled plasma-atomic absorption spectroscopy (ICP/AAS). BET surface areas and pore-size distributions were determined by N₂ adsorption on an ASAP2010M instrument (Micromeritics). The pore-size distributions were calculated by the advanced BJH method from desorption branches of the isotherms. The samples were degassed at 400 °C in vacuum prior to measurements. XRD analysis was performed on a X'Pert instrument (Philips) using Cu K α radiation (40 kV, 40 mA). The electron probe microanalyser SX-100 (Cameca, France) working in the scanning electron microscopy (SEM) mode was used for imaging the support surfaces. The W cathode at 20 kV voltage was applied during the measurement on the samples coated with thin layer of gold. Transmission electron microscopy (HRTEM/SAED) was performed on a JEM 3010 electron microscope (Jeol) equipped with LaB₆ cathode and operating at 300 kV. The samples were grounded in an agate mortar, suspended in ethanol and droplets of the suspensions were placed on a copper grid. Several images of different particles were taken for each support and the two were finally selected as typical ones. The ²⁷Al MAS NMR spectra were recorded at 130.33 MHz on an Bruker Avance 500 WB/US NMR spectrometer (Germany) using a magic angle spinning (MAS) frequency of 11 kHz. The fine-ground samples (80 mg) were placed in 4 mm ZrO₂ rotor. The pulse length was 0.8 μ s and the repetition delay of 2 s. ²⁷Al NMR chemical shifts are reported relative to Al(NO₃)₂·6H₂O (0.0 ppm). The spectra were decomposed by the computer program package DmFit.

The Pt dispersion in majority of the reduced catalysts was determined by pulse H₂ adsorption in a home-made apparatus with thermal conductivity detection (TCD) at 22 °C as described else-

where [20]. The catalyst (500 mg) was reduced by H_2 at $400^\circ C$, purged by N_2 at $400^\circ C$ for 0.5 h and cooled to $22^\circ C$ in N_2 . It was then titrated by pulses of H_2 . The $H:Pt = 1:1$ stoichiometry was adopted according to Anderson and Pratt [21]. Two samples were measured by CO sorption, the 0.85PtO-11, available in small amount and 0.95PtC-34, showing the H/Pt ratio exceeding unity. The CO chemisorption was carried out on a commercial Autochem 2920 instrument (Micromeritics). 50 mg of catalyst was reduced by 5% H_2 in Ar at $400^\circ C$, purged by He at $400^\circ C$ for 1 h and cooled to $0^\circ C$ in He. It was then titrated by pulses of 5% CO in He. The CO:Pt = 1:1 stoichiometry was used for calculation of Pt dispersion. It was confirmed that both methods gave similar dispersion values on a standard Pt catalyst. CO sorption gave for a Pt/MSA (0.52% Pt) value $CO/Pt = 0.80$, i.e. very close to that found by H_2 sorption $H/Pt = 0.87$ on this sample previously [12].

2.3. Catalytic tests

2.3.1. Skeletal isomerization of cyclohexene and cracking of cumene

The catalytic activity of supports in the isomerization of cyclohexene (CH) was tested at $240^\circ C$ and 0.5 MPa in a flow microreactor with fixed catalyst bed described in detail elsewhere [22]. The supports (20×10^{-6} kg) were in situ activated by H_2 at $400^\circ C$ for 0.5 h. After the catalyst temperature had decreased to $240^\circ C$, the feed (200 ppm CH in H_2) was introduced by a 6-port valve with the flow rate of 150 ml/min. The CH conversions into 1-methylcyclopentene (1-MCPE) were evaluated from compositions of the feed and of the reaction products analysed on-line in 15 min intervals during 4 h on stream. A gas chromatograph Agilent 4890D operated with FID detector and 30 m capillary DB-5 column (0.25 mm) at $50^\circ C$.

The activity of the supports in cumene (CU) cracking was tested at temperatures 300 – $400^\circ C$ and pressure of 0.5 MPa in the same apparatus. The weight, supports pretreatment and the procedure was essentially the same as for the isomerization. H_2 was passed at the flow rate of 150 ml/min through a pressure saturator filled with CU. The CU content in the H_2 stream was 200 ppm. The conversions into benzene and propylene were evaluated from compositions of the feed and reaction products analysed in 20 min intervals during 3–5 h on stream. The analyses were performed on a 30 m capillary DB-5 column (0.25 mm) at $115^\circ C$. Analyses of the heavier reaction products, which were condensed and trapped in the run with MSA11, were performed separately at $170^\circ C$.

2.3.2. HDS of thiophene

The activity of the Pt catalysts in HDS of thiophene (TH) was evaluated in another flow microreactor system with fixed catalyst bed at temperature $320^\circ C$ and overall pressure 2 MPa. The feed, generated by passing H_2 through a pressure saturator filled with TH, contained 240 ppm of TH in H_2 of the flow rate of 150 ml/min. The rate of the feed was kept constant $F_{TH} = 9.7 \times 10^{-5}$ mol $_{TH}$ /h. The catalyst amount W was 6 – 15×10^{-6} kg. Before tests, the catalysts were in situ activated by their reduction in H_2 at atmospheric pressure under heating to $400^\circ C$ (ramp $5^\circ C/min$) and keeping at this temperature for 1 h. Then the temperature was decreased to $320^\circ C$ and hydrogen was replaced by the feed via a 6-port valve. The samples of the feed and the reaction mixture were taken in 30 min intervals. The steady state was usually achieved within 2 h on stream, and the representative composition of the reaction products was calculated from several subsequent analyses. The on-line analyses were performed on a gas chromatograph HP 5890 equipped with FID detector and 3.5 m glass column packed with CarboPack B 60/80 4% Carbowax 20 M (Supelco) operating at $125^\circ C$. The products of thiophene HDS were C_4 hydrocarbons, H_2S and tetrahydrothiophene (THT). The steady state HDS activities were expressed by overall TH conversion, x_{TH} , conversion of TH in THT, x_{THT} , and in C_4

hydrocarbons, x_{C_4} . The pseudo-first-order rate constants k_{TH} were calculated according to Eq. (1)

$$k_{TH} = - \left(\frac{F_{TH}}{W} \right) \ln (1 - X_{TH}) \quad (1)$$

The x_{TH} was defined as $1 - n/n_{TH}^0$, where n_{TH}^0 and n_{TH} are numbers of moles of TH in the feed and the reaction products, respectively. The $x_{i,j}$, where $i = THT$ and $j = C_4$, were defined as $n_{i,j}/n_{TH}^0$, where $n_{i,j}$ are the numbers of moles of i,j in the reaction products. The percentage of deactivation (Deact.) was expressed as $100(x_{TH}^0 - x_{TH})/x_{TH}^0$, where x_{TH}^0 is initial TH conversion.

2.3.3. HDS of benzothiophene

HDS of benzothiophene (BT) was carried out in the gas phase in a flow microreactor (i.d. 3 mm) with the fixed catalyst bed at $330^\circ C$ and 1.6 MPa of overall pressure described elsewhere [23]. The liquid feed was fed by a Waters 510 HPLC pump into evaporator section connected to the reactor and separation systems. The feed rate F_{BT} was 7.7×10^{-3} mol $_{BT}$ /h and the feed composition was kept constant as 16, 200 and 1384 kPa of BT, decane and hydrogen, respectively. The catalyst ($W = 40 \times 10^{-6}$ kg) was diluted with inert α -Al₂O₃ (Alfa Aesar) to form a 30 mm bed. Before measurements, the catalysts were in situ re-activated by reduction in H_2 at atmospheric pressure under heating to $400^\circ C$ (ramp of $4^\circ C/min$) and keeping at this temperature for 1 h. The samples of the condensed reaction mixture were taken at 1–3 h on stream and analysed on a HP 6890 gas chromatograph equipped with a 30 m capillary HP-5 column (0.53 mm). The analyses were performed using a temperature program starting at $130^\circ C$ (3 min) followed by a ramp $10^\circ C/min$ up to $180^\circ C$. The reaction products were ethylbenzene (EB), H_2S and dihydrobenzothiophene (DHBT). The steady state HDS activities of the catalysts were expressed by overall BT conversion x_{BT} , conversion of BT to DHBT, x_{DHBT} , and to EB, x_{EB} . The conversions and the pseudo-first-order rate constants k_{BT} were calculated analogously as those for TH.

3. Results and discussion

3.1. Properties of supports

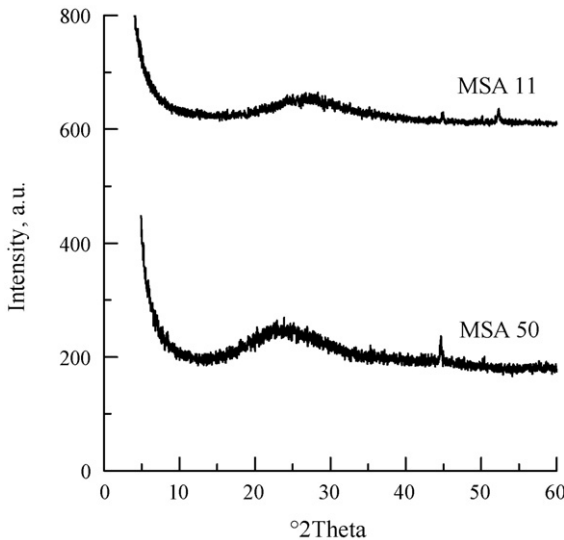
The leaching of MSA with different amounts of nitric acid gave several samples, which were characterized by their composition, surface areas, texture and by activities in acid catalyzed reactions. In order to reduce the number of supports with similar properties, only three samples differing significantly in Al₂O₃ content, BET surface area and acidity were selected for further work (MSA50, 34 and 11). They were characterized in more detail (²⁷AL MAS NMR, SEM, HRTEM) and used for preparation of catalysts. Table 1 summarizes the composition and properties of the all MSA samples and HY support. The alumina content in the MSA samples was gradually reduced from 50 to 11 wt.% by acid leaching and this process was accompanied by parallel extraction of the residual sodium. The X-ray diffraction showed that neither MSA50 nor MSA11 possess distinct diffraction lines, showing amorphous character of these materials (Fig. 1). On the other hand, the well developed diffraction lines of the HY support are shown in Fig. 2, being in an agreement with the literature [24,25].

Fig. 3 shows the nitrogen adsorption isotherms for the parent MSA50 and modified MSA34 and MSA11. The type of the isotherm was the same for both the leached and the original sample. The inset in Fig. 3 shows that the pore-size distributions remained very narrow with mean pore diameters 3.5, 4.4 and 3.5 nm for MSA50, MSA34 and MSA11, respectively. It can be concluded that despite of the removal of considerable weight fractions of Al₂O₃ from MSA50, more significant changes or even destruction of the mesoporous

Table 1

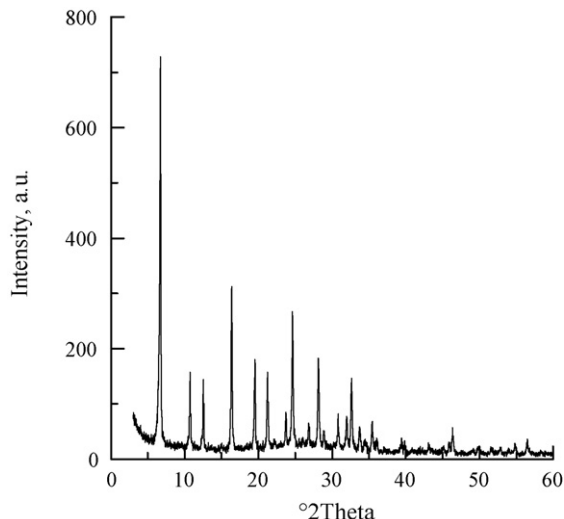
Composition, textural properties and steady state activities of supports in cyclohexene and cumene conversions.

Support	Content (wt.%)		S_{BET} (m ² /g)	V_p (cm ³ /g)	x_{CH}^{240}	x_{CU}^{400}
	Al ₂ O ₃	Na				
MSA50	50	0.18	491	0.61	0.28	0.25
MSA34	34	0.03	536	0.64	0.64	0.63
MSA28	28	n.d. ^b	549	0.63	0.60	0.56
MSA14	14	n.d. ^b	584	0.53	0.65	0.67
MSA11	11	<0.01	575	0.51	0.59	0.68
HY	14 ^a	0.40	216	0.06	0.14	1.00 (0.96) ^c

^a Corresponds to Si/Al=5.^b Not determined.^c At reaction temperature 300 °C.**Fig. 1.** X-ray diffraction of MSA50 and MSA11 supports.

structure have not been observed. The same holds for MSA28 and MSA14 (not shown).

The BET surface areas of the MSA samples gradually increased with progressive leaching up to about 580 m²/g (Table 1). The surface of the mesopores of all the samples was typically above 350 m²/g, forming at least 65% of the BET surface areas. The total

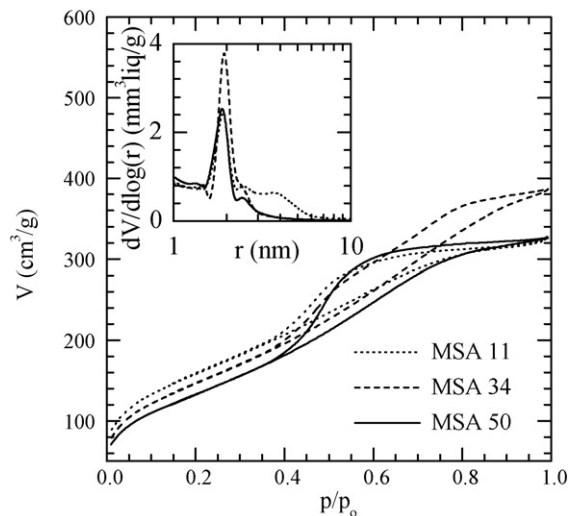
**Fig. 2.** X-ray diffraction of HY support.

pore volume remained almost the same and only little higher values were found for the samples containing around 30% Al₂O₃.

The surface area of the powdered HY was 580 m²/g, close to the value reported in the literature [24]. However, this value was substantially reduced during the pelletizing procedure (Table 1). The main reason was most likely too high pressure of 2 MPa necessary for the preparation of sufficiently hard particles.

The SEM images of the MSA50, MSA34 and MSA11 are shown in Fig. 4. In contrast to the surface of MSA50, progressive erosion on MSA34 and MSA11 is well apparent. The appearance of the cavities of up to 10 µm can most likely be explained by ablation of the alumina-rich clusters. The HRTEM images of MSA50 and MSA11 samples are shown in Fig. 5. Before measurements, the amorphous character of the both samples was again confirmed by the SAED (selected area electron diffraction), being in accordance with the results of the preceding X-ray diffraction. A fairly high occurrence of fibrous particles was well apparent in the original MSA50 (Fig. 5a). They were observed already in our previous work [10] and could most likely be ascribed, in accordance with the literature, to pseudoboehmite phase [26]. These particles completely disappeared after acid leaching, as obvious from Fig. 5b.

The ²⁷Al MAS NMR spectra of the MSA50, MSA34 and MSA11 are depicted in Fig. 6. The maxima of the main peaks are located at about 7, 32 and 56 ppm. The signals at 7 and 56 ppm correspond to the aluminum in the octahedral (Al_{oct}) and tetrahedral (Al_{tet}) coordination, respectively, while the signal at 32 ppm is usually ascribed to the pentacoordinated aluminum (Al_{pent}) [27,28]. The amounts of these species evaluated by deconvolution of the spectra are summarized in Table 2. The original MSA50 contains three species, with

**Fig. 3.** Nitrogen adsorption isotherms and pore-size distributions of MSA50, MSA34 and MSA11.

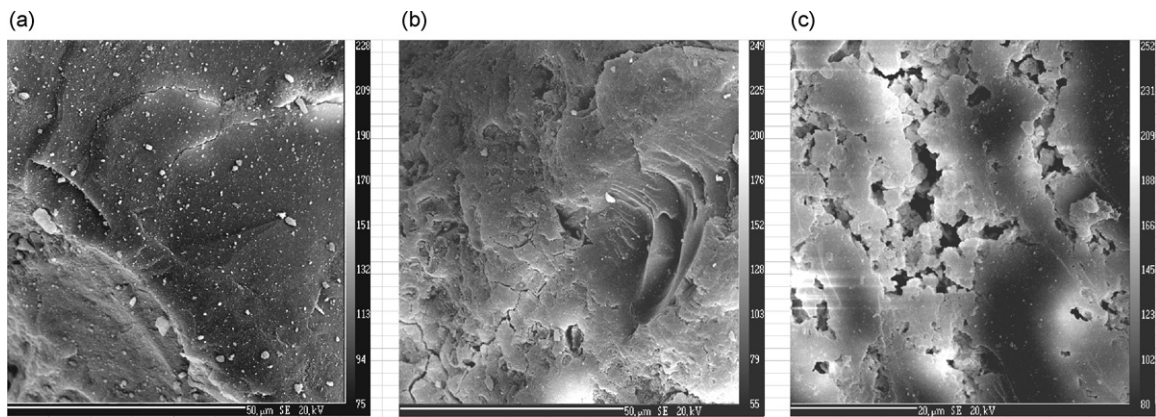


Fig. 4. SEM images of MSA50 (a), MSA34 (b) and MSA11 (c).

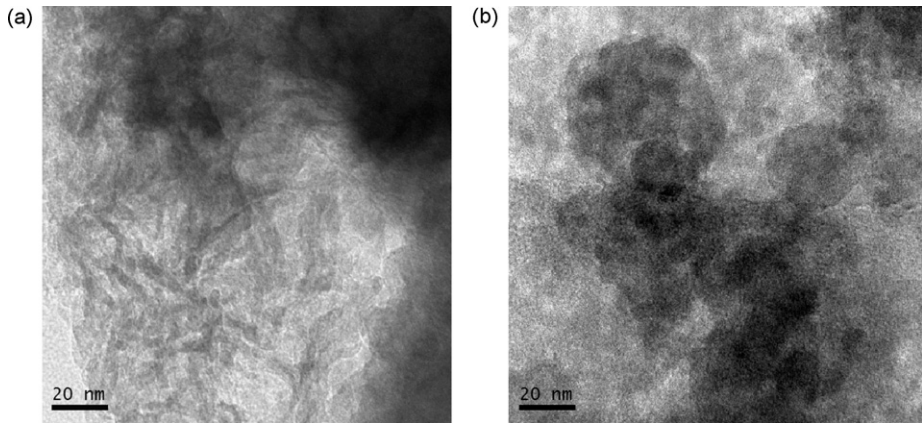


Fig. 5. HRTEM images of MSA50 (a) and MSA11 (b).

Al_{oct} as dominant. The values for this support determined in the present work are almost the same as those found by us earlier with different deconvolution procedure, which were 21, 6 and 73% [10]. Data in Table 2 show that leaching of the MSA50 led to the complete elimination of the Al_{pent} species, a partial removal of the Al_{oct} species and about twofold enrichment by Al_{tet} . The reduction of the

amounts of Al_{pent} and Al_{oct} species, i.e. the extra-framework aluminum in MSA50, well corroborates the conclusion concerning the removal of pseudoboehmite phase observed by HRTEM.

3.2. Activity of supports in isomerization of cyclohexene and cracking of cumene

The acidity of the supports was characterized by catalytic activities in two acid catalyzed reactions, skeletal isomerization of cyclohexene (CH) and cracking of cumene (CU). Brønsted acidity is required for both reactions [29] and CU cracking is believed to require stronger sites than CH isomerization [30]. The conversions of both compounds were thus considered as simple indices of the support acidities for the purpose of this work. The activities of all the samples are summarized in Table 1.

CH was transformed into 1-MCPE and small amounts of 3- and 4-isomers, traces of cyclohexane and lighter products over the MSA samples at 240 °C. At this temperature, transformation of CU over the MSA samples gave low conversions. With exception of the HY, which was very active already at 300 °C, the reasonable conversions over MSA samples were obtained at 400 °C, similarly as in

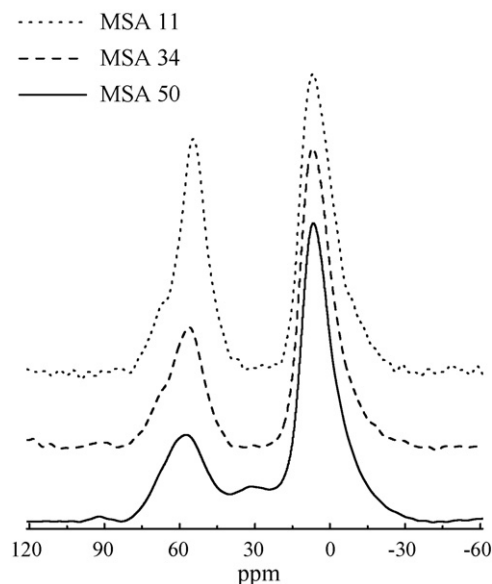


Fig. 6. ^{27}Al MAS NMR spectra of MSA50, MSA34 and MSA11.

Table 2
Relative abundance of Al species evaluated by ^{27}Al MAS NMR.

Support	Al_{tet} (%)	Al_{pent} (%)	Al_{oct} (%)
MSA50	24 (21) ^a	8 (6) ^a	68 (73) ^a
MSA34	30	0	70
MSA11	41	0	59

^a Values in parentheses taken from Ref. [10].

Table 3

Effect of leaching of residual Na on support steady state activity in cyclohexene and cumene conversions.

Treatment of MSA50	Na content (wt. %)	x_{CH}^{240}	x_{CU}^{400}
None	0.18	0.28	0.25
Ion exch. 4 h	0.11	0.64	0.25
Ion exch. 2 h \times 20 h	0.08	0.56	0.28

other studies [27,29]. Dealkylation into benzene and propylene represented a major part of CU transformation, accompanied by the formation of smaller amounts of propylbenzene, ethylbenzene and diisopropylbenzenes. These by-products were found earlier in the other studies performed over ASA and different zeolites as well [31]. It is of interest that the HY possessing an exceptional cracking activity showed only poor isomerization activity. This can hardly be explained by steric hindrances for the reacting molecules, since CH and 1-MCPE molecules are smaller than that of CU. It seems more likely that also the character of Brønsted acid sites or their density play coessential roles. Nevertheless, regardless of this point, it can be concluded that the reduction of Al_2O_3 content in MSA led to the great improvement of the activities in these reactions. The data in Table 1 suggest that the CH isomerization activity went through a mild maximum between 10 and 30% Al_2O_3 . The cracking activity continuously increased with progressive leaching, so that MSA14 and MSA11 samples were the most active. The modified samples thus showed clearly higher and stronger acidities than the original MSA50.

The leaching by diluted HNO_3 was accompanied by a partial extraction of the residual sodium (Table 1). Sodium is known efficient poison of acid sites, and thus the additional experiments were performed in order to find whether the removal of the part of Al_2O_3 or the reduction of sodium content were decisive for the formation of strong acidity. For this purpose, MSA50 was repeatedly ion-exchanged with the AN solutions and after transformation into the acidic form again tested in both reactions. In contrast to the acid leaching, the ion-exchange removes selectively sodium, keeping the Al_2O_3 content intact. The results are shown in Table 3. The decrease of the sodium amount to about one half had a great positive effect on CH isomerization, but almost none on CU cracking. This showed that the acid sites released by sodium removal, at least down to around 0.08% Na, were able to catalyze only CH isomerization, demonstrating by this way the lower acid strength involved. This result suggests that the strong acidity of the acid leached samples could better be ascribed to the removal of Al_2O_3 and not of sodium. This conclusion is in agreement with the greater fraction of the Al_{tet} present in the more leached samples, which is often related to the strong acidity of ASA [27,28].

As already stated, the leaching of the MSA significantly increased their BET surface area and activities of the supports in isomerization and cracking reactions, i.e. their acidity. We therefore conclude, that partial removal of the free non-acidic Al_2O_3 phase from MSA has analogous and cleaning up effect as the removal of the EFAL from zeolites. This is obviously the main reason for the unblocking of the strong acid sites primarily present in the silica–alumina phase.

3.3. Pt dispersion in the catalysts

Four supports were selected as representative for the preparation of Pt catalysts, the original MSA50, two modified MSA34, MSA11 and HY. The hydrogen (or CO) uptake and Pt dispersion of the reduced catalysts is given in Table 4. The majority of dispersion values, expressed as H/Pt or CO/Pt ratios, varied between 0.20–0.91. An exceptional behavior, i.e. the value H/Pt = 1.36 was shown by the sample 0.95PtC-34. We speculate about this being due to hydrogen spillover between Pt and the MSA34 support,

Table 4

Hydrogen (or CO) uptake and dispersion of reduced Pt catalysts.

Catalyst	V_{ads} (ml/g _{cat})	H(CO)/Pt
1.30PtC-50	0.47	0.64
0.95PtC-34	0.74, 0.22 ^a	1.36, 0.20 ^a
0.92PtN-34	0.20	0.38
0.64PtC-11	0.27	0.72
0.92PtN-11	0.25	0.47
1.70PtN-11	0.30	0.31
0.85PtO-11	0.89 ^a	0.91 ^a
1.52PtO-11	0.46	0.53
0.98PtC-HY	0.21	0.37

^a Determined by CO sorption.

similarly as observed Satoh et al. for hydrogen on $\text{Pt}/\text{SO}_4^{2-}-\text{ZrO}_2$ catalyst [32]. It was proposed that hydrogen dissociated on Pt and migrated to oxygen atoms in the vicinity of Lewis acid sites. In order to eliminate such effect, the Pt dispersion was also evaluated by CO which gave the value CO/Pt = 0.20. This result further supports our assumption concerning the hydrogen spillover and suggests, that the real Pt dispersion in 0.95PtC-34 is substantially lower than shown by H/Pt value. The data in Table 4 suggest that H_2PtCl_6 as the precursor gives good Pt dispersion on the support with the highest Al_2O_3 content (MSA 50). On more siliceous MSA11 sample, very high dispersions were achieved with $\text{Pt}(\text{NH}_3)_4(\text{OH})_2$, around twofold over those achieved with $\text{Pt}(\text{NH}_3)_4\text{Cl}_2$ at the comparable Pt loadings. This is obviously connected with the strength of interaction between the Pt precursors and the support, in agreement with the previous adsorption studies of Pt compounds on different alumina and silica samples [33,34 and references therein].

3.4. Activity of Pt catalysts in HDS of thiophene

The basic conversion data and the rate constants k_{TH} are summarized in Table 5. The activities of the $\text{CoMo}/\text{Al}_2\text{O}_3$, 0.98PtC-HY and the 1.30PtC-50 catalysts were stable during several hours of run. However, some deactivation was observed during the first 4 h on stream over the Pt catalysts prepared from both acid leached supports. HDS over all Pt catalysts was accompanied by the formation of THT, as observed over different zeolite supported Pt catalysts by other authors [35,36]. The very high activity of the 1.52PtO-11 at 320 °C led to almost quantitative x_{TH}^0 even at the lowest catalyst charge; this sample was therefore tested also at the lower temperature of 280 °C.

3.4.1. Effect of support and Pt precursor on thiophene HDS activity

The effect of the support of Pt catalysts prepared from H_2PtCl_6 on thiophene HDS activity is shown in Table 6. In order to eliminate the different Pt amounts and dispersions in the catalysts, the activities were expressed per mol of the deposited Pt as the specific activities and normalized to the accessible Pt atoms as the turnover frequencies, respectively. Data in Table 6 show that the specific activities were substantially higher for the catalysts prepared from MSA34 and MSA11 as compared to MSA50 and HY. The TOF_{TH} values show an increasing trend parallel to increasing acidity in the order MSA50 < MSA11 < HY and support the idea of participation of strong Brønsted sites in thiophene adsorption and HDS, as already proposed by Japanese workers [6–9]. However, the highest TOF_{TH} value, calculated from dispersion CO/Pt = 0.20, was shown by 0.95PtC-34 catalyst. An exceptional hydrogen uptake on this sample was ascribed to the hydrogen spillover and one can speculate that it could be the reason for very high TOF_{TH} as well. Hydrogen activated on Pt can migrate and create new Brønsted sites or be delivered in a greater extent to the adsorbed TH species, acceler-

Table 5

Conversion data and thiophene HDS rate constants.

Catalyst	Reaction temperature (°C)	W (mg)	x_{TH}	x_{THT}	x_{C_4}	x_{TH}^0	Deact. (%)	k_{TH} (mol _{TH} /h kg _{cat})	k_{TH}^0 (mol _{TH} /h kg _{cat})
1.30PtC-50	320	7.4	0.71	0.11	0.59	(0.73) ^a	3	16.6	(18.0) ^a
0.95PtC-34	320	6.6	0.75	0.07	0.68	(0.87)	14	19.6	(28.5)
0.92PtN-34	320	9.9	0.65	0.37	0.28	(0.79)	18	13.0	(18.9)
0.64PtC-11	320	12.5	0.80	0.04	0.76	(0.92)	13	12.1	(18.7)
0.92PtN-11	320	8.6	0.79	0.13	0.66	(0.89)	11	21.0	(29.7)
1.70PtN-11	320	8.1	0.87	0.11	0.73	(0.94)	7	29.2	(40.5)
0.85PtO-11	320	7.0	0.77	0.05	0.71	(0.91)	15	25.4	(39.8)
1.52PtO-11	320	5.6	0.93	0.04	0.86	(0.99)	6	67.5	(107.1)
0.98PtC-HY	320	9.9	0.77	0.26	0.51	(0.77)	0	13.7	(13.7)
CoMo	320	6.3	0.78	0.00	0.78	(0.78)	0	24.5	(24.5)
1.52PtO-11	280	5.6	0.58	0.32	0.26	n.d. ^b	–	20.2	–
CoMo	280	6.3	0.33	0.00	0.33	(0.33)	0	6.5	(6.5)

^a Initial activity in parentheses.^b Not determined.**Table 6**

Effect of support on steady state specific activity and turnover frequency in thiophene HDS 320 °C, 2 MPa.

Catalyst	Support	k_{TH} (mol _{TH} /(h mol _{Pt}))	TOF _{TH} (1/h)
1.30PtC-50	MSA50	249	390
0.95PtC-34	MSA34	402	2010 ^a
0.64PtC-11	MSA11	369	510
0.98PtC-HY	HY	272	740

^a Calculated from value CO/Pt = 0.20.

ating the rate of TH transformation. Table 7 shows the effect of Pt precursor on the specific thiophene HDS activity and TOF_{TH} for MSA11 supported catalysts. H₂PtCl₆ and Pt(NH₃)₄Cl₂ gave the catalysts with lower specific activities per mol of deposited Pt than Pt(NH₃)₄(OH)₂. Similarly, the lowest TOF_{TH} value was also found for the 0.64PtC-11 sample prepared from H₂PtCl₆, while the highest TOF_{TH} in this series of catalysts was obtained with Pt(NH₃)₄(OH)₂. This compound was by far the best precursor for MSA11 support, giving the catalysts with high Pt dispersions and superior activities in thiophene HDS.

3.4.2. Effect of Pt dispersion on THT selectivity

The content of THT as the reaction intermediate was constant during several hours on stream showing that hydrogenation route significantly contributes in transformation of TH over Pt catalysts. Fig. 7 shows the x_{THT} values plotted against the Pt dispersion of the catalysts on which approximately the same x_{TH} values were achieved. These data clearly show that the content of THT is strongly reduced on increasing Pt dispersion, i.e. with the smaller size of metal particles. This result is in agreement with the known fact that smaller metal particles contain more edges and defect sites than the larger ones. Their presence generally favours hydrogenolysis, while larger metal particles facilitate hydrogenation. Niquille-Röthlisberger and Prins demonstrated this effect in the case of HDS of 4,6-DMDBT over reduced Pt/ASA catalysts with different dispersion [4]. They showed that Pt dispersion significantly changed

the selectivity of the reaction; i.e. the ratio of hydrogenation pathway to direct C–S bond hydrogenolysis (DDS). The higher DDS/HYD ratio was found for Pt/ASA having the higher Pt dispersion. One can therefore assume that the same effect plays a role over Pt/MSA catalysts in the present work as well. In contrast to the Pt catalysts, CoMo/Al₂O₃ did not produce THT at the same experimental conditions. In this case, thiophene HDS might proceed almost exclusively by DDS, as in the study by Leglise et al. [37], carried out under similar experimental conditions (340 °C, 3 MPa).

3.4.3. Activity of catalysts in HDS of benzothiophene

The MSA11 supported catalysts, which were most active in HDS of TH, were also tested with BT and compared with the HY supported sample and CoMo/Al₂O₃. The conversion data, rate constants for BT disappearance k_{BT} and TOF_{BT} values are given in Table 8. A small activity decay around 10% was found between 1 and 3 h of catalytic run; thus only data after 3 h on stream are given. The samples, most active per weight amount, were again the 1.52PtO-11 and 1.70PtN-11 and the least active was the 0.98PtC-HY. The order of HDS activities k_{BT} was therefore almost the same as that found with TH (Table 5). The trend in the TOF_{BT} values was the same for four samples as that found for TOF_{TH}; 1.70PtN-11 ≈ 0.92PtN-11 > 0.98PtC-HY > 0.85PtO-11. The exception was only the 1.52PtO-11, due to very high

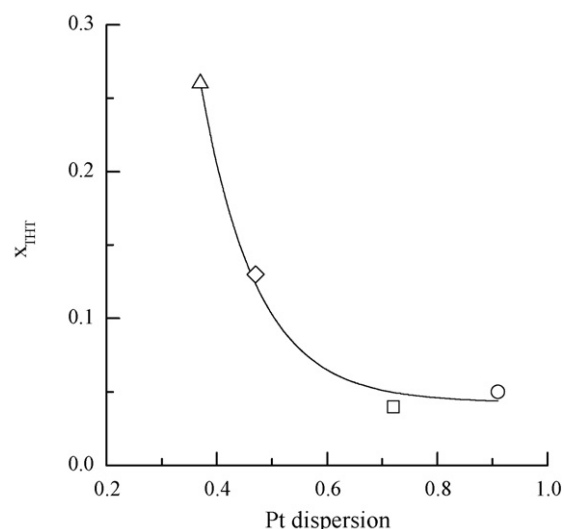


Fig. 7. THT formation in thiophene HDS as a function of Pt dispersion. Catalysts: PtC-HY (Δ), PtN-11 (\diamond), PtO-11 (\circ), PtC-11 (\square). Comparison at $x_{\text{TH}} = 0.77$ –0.80.

Table 7

Effect of Pt precursor on steady state specific activity and turnover frequency in thiophene HDS 320 °C, 2 MPa.

Catalyst	Precursor	k_{TH} (mol _{TH} /(h mol _{Pt}))	TOF _{TH} (1/h)
0.64PtC-11	H ₂ PtCl ₆	369	510
0.92PtN-11	Pt(NH ₃) ₄ Cl ₂	445	950
1.70PtN-11	Pt(NH ₃) ₄ Cl ₂	335	1080
0.85PtO-11	Pt(NH ₃) ₄ (OH) ₂	583	640
1.52PtO-11	Pt(NH ₃) ₄ (OH) ₂	867	1640

Table 8

Conversion data and benzothiophene HDS rate constants 330 °C, 1.6 MPa; catalyst weight 40 mg.

Catalyst	X_{BT}	X_{DHBT}	X_{EB}	k_{BT} (mol _{BT} /(h kg _{cat}))	TOF _{BT} (1/h)
0.92PtN-11	0.35	0.18	0.17	82	3700
1.70PtN-11	0.41	0.20	0.21	102	3780
0.85PtO-11	0.31	0.13	0.18	73	1840
1.52PtO-11	0.46	0.19	0.27	119	2880
0.98PtC-HY	0.27	0.15	0.12	61	3280
CoMo	0.42	0.08	0.34	107	–

activity in thiophene HDS. Transformation of BT was accompanied by the formation of significant amounts of DHBT. Its formation over all the Pt catalysts was about two times higher as compared to CoMo/Al₂O₃. The catalysts prepared from Pt(NH₃)₄Cl₂ gave more DHBT than those prepared from Pt(NH₃)₄(OH)₂. This trend is the same as for THT formation (Table 5) and can again be ascribed to different Pt dispersion, already discussed in Section 3.4.2. The catalysts prepared from Pt(NH₃)₄Cl₂ showed lower Pt dispersion (Table 4) and thus give higher HYD/hydrogenolysis ratio and more DHBT than samples originated from Pt(NH₃)₄(OH)₂. Larger amounts of hydrogenated intermediates suggest that there is a greater contribution of HYD pathway at the expense of direct desulfurization (DDS).

3.4.4 Effect of Pt loading and comparison with CoMo/Al₂O₃

The rate constants for TH and BT disappearance over the Pt catalysts, relative to those for CoMo/Al₂O₃, k_{REL} , are plotted against Pt loading in Fig. 8. Some recent studies showed that thiophene HDS activities increased almost linearly with Pt loading up to around 2 wt. % Pt on FSM-16, Al-SBA-15 [7,9] and our MSA [12]. The data obtained in the present work were thus also interpolated by the straight lines. Fig. 8 shows that the activity of the catalysts prepared from Pt(NH₃)₄(OH)₂ and Pt(NH₃)₄Cl₂ were fairly proportional to Pt loadings for both model compounds. Moreover, the k_{REL} for the 0.98PtC-HY and catalysts prepared from Pt(NH₃)₄Cl₂ were almost the same for TH and BT reactions. It is interesting that both samples prepared from Pt(NH₃)₄(OH)₂ showed great differences in TH and BT reactions. In the former, the 1.52PtO-11 was almost three times more active than CoMo/Al₂O₃, while only slightly better for BT. The reason for this behavior is not quite clear. We speculate that this

difference could be related to the higher Pt dispersion of these samples, which should lead to the greater contribution of the C–S bond hydrogenolysis and lower HYD, being most likely nonessential for thiophene HDS. It has recently been shown, that BT transformation on Pt/zeolite catalysts was mainly facilitated by its easier hydrogenation [35]. However, the HYD proceeds more easily on larger metal particles [4] which may be a certain handicap for BT reaction over the catalysts prepared from Pt(NH₃)₄(OH)₂. One can also speculate with larger dimension of BT molecule in contrast to TH, which theoretically could lead to slower diffusion and lower accessibility of active sites of 1.52PtO-11. However, we suppose that relatively low amount of well dispersed Pt can hardly block the pores with orifice around 3.5 nm. Moreover, some recent studies showed that mesoporous MCM-41 with pore diameters around 3 nm gave highly active NiMo catalysts for HDS of DBT [19,24]. Contreras et al. [35] did not observe apparent diffusion limitations in HDS of TH, BT and DBT even on zeolite (HFUA) supported Pt catalyst with pore dimensions 0.74 nm × 0.74 nm. Taking into account these results, it can be expected that molecules like BT and DBT should easily enter the 3.5 nm pores of MSA11 and that the lower BT activity of both PtO-11 based catalysts is most likely not in a relation to their texture.

A rough estimation of data in Fig. 8 shows that the loading giving the catalyst in thiophene HDS as active as weight equivalent of CoMo/Al₂O₃, is attained already at 0.6 wt.% Pt for Pt(NH₃)₄(OH)₂ on MSA11. This seems to be much less than the Pt loadings reported in other studies [7,9]. However, we are well aware of the fact that different reaction conditions and origin of CoMo/Al₂O₃ catalysts make such a comparison only approximate. With respect to BT conversion, loadings at around 1.2 wt.% Pt deposited by means of Pt(NH₃)₄(OH)₂ or Pt(NH₃)₄Cl₂ on MSA11 gave the activities equal to the weight amount of CoMo/Al₂O₃.

4. Conclusions

Acid leaching of the mesoporous silica–alumina (MSA) containing 50% Al₂O₃ with HNO₃ led to materials with the lower Al₂O₃ contents 10–30%, strong acidities and higher BET surface areas. The leaching removed the extra-framework Al_{pent} and part of the Al_{oct} species and increased the proportion of Al_{tet} species. The higher acidity of the modified supports positively influenced the activity of the reduced Pt catalysts in thiophene HDS. The kind of the Pt precursor was an additional important factor, strongly affecting the catalyst activity. The most active HDS catalyst was obtained by deposition of Pt(NH₃)₄(OH)₂ on MSA containing 11% Al₂O₃. The catalyst containing 1.5 wt.% Pt was about 3 and 5 times more active in thiophene HDS than weight equivalents of CoMo/Al₂O₃ and the reduced Pt/HY, respectively. In benzothiophene transformation, its activity was relatively lower than in thiophene HDS, but still exceeding the activities of CoMo/Al₂O₃ and Pt/HY.

Acknowledgement

The financial support of the Czech Science Foundation (Grant 104/09/0751) is gratefully acknowledged.

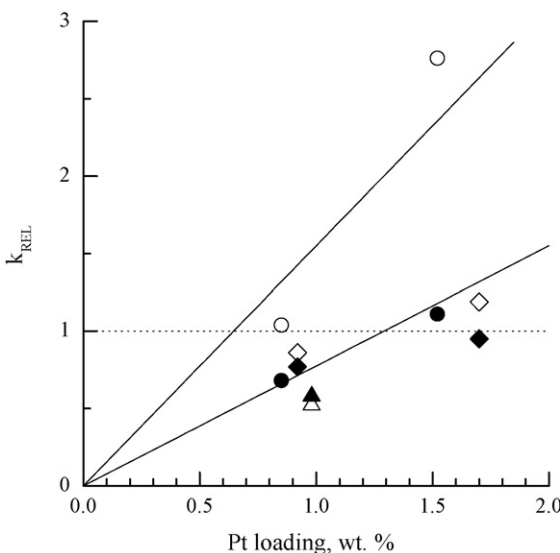


Fig. 8. HDS activity of Pt catalysts relative to CoMo/Al₂O₃ as a function of Pt loading. Catalysts: PtO-11 (○, ●), PtN-11 (◊, ♦), PtC-HY (Δ, ▲). Thiophene (open points), benzothiophene (full points).

References

- [1] R. Navarro, B. Pawelec, J.L.G. Fierro, P.T. Vasudevan, J.F. Cambra, P.L. Arias, *Appl. Catal. A* 137 (1996) 269–286.
- [2] W.R.A.M. Robinson, J.A.R. van Veen, V.H.J. de Beer, R.A. van Santen, *Fuel Process. Technol.* 61 (1999) 89–101.
- [3] W.R.A.M. Robinson, J.A.R. van Veen, V.H.J. de Beer, R.A. van Santen, *Fuel Process. Technol.* 61 (1999) 103–116.
- [4] A. Niquille-Röthlisberger, R. Prins, *Catal. Today* 123 (2007) 198–207.
- [5] M.F. Williams, B. Fonté, C. Woltz, J.A.R. van Veen, J.A. Lercher, *J. Catal.* 251 (2007) 497–506.
- [6] M. Sugioka, F. Sado, T. Kurosaka, W. Wang, *Catal. Today* 45 (1998) 327–334.
- [7] M. Sugioka, L. Andalaluna, S. Morishita, T. Kurosaka, *Catal. Today* 39 (1997) 61–67.
- [8] Y. Kanda, T. Kobayashi, Y. Uemichi, S. Namba, M. Sugioka, *Appl. Catal. A* 308 (2006) 111–118.
- [9] Y. Kanda, T. Aizawa, T. Kobayashi, Y. Uemichi, S. Namba, M. Sugioka, *Appl. Catal. B: Environ.* 77 (2007) 117–124.
- [10] Z. Vít, O. Šolcová, *Micropor. Mesopor. Mater.* 96 (2006) 197–204.
- [11] D. Gulková, Z. Vít, *Stud. Surf. Sci. Catal.* 162 (2006) 489–496.
- [12] D. Gulková, Y. Yoshimura, Z. Vít, *Appl. Catal. B: Environ.* 87 (2009) 171–180.
- [13] J.P. Reymond, J.F. Quinson, *Stud. Surf. Sci. Catal.* 128 (2000) 623–631.
- [14] A. Gola, B. Rebours, E. Milazzo, J. Lynch, E. Benazzi, S. Lacombe, L. Delevoye, C. Fernandes, *Micropor. Mesopor. Mater.* 40 (2000) 73–83.
- [15] J.T. Miller, P.D. Hopkins, B.L. Meyers, G.J. Ray, R.T. Roginski, G.W. Zajac, N.H. Rosenbaum, *J. Catal.* 138 (1992) 115–128.
- [16] L.D. Fernandes, P.E. Bartl, J.L.F. Monteiro, J.G. da Silva, S.C. de Menezes, M.J.B. Cardoso, *Zeolites* 14 (1994) 533–540.
- [17] S.M.C. Menezes, V.L. Camorim, Y.L. Lam, R.A.S. San Gil, A. Bailly, J.P. Amoreux, *Appl. Catal. A: Gen.* 207 (2001) 367–377.
- [18] G. de la Puente, E. Falabella Souza-Aguiar, A.F. Costa, U. Sedran, *Appl. Catal. A: Gen.* 242 (2003) 381–391.
- [19] X. Li, A. Wang, Y. Wang, Y. Chen, Y. Liu, Y. Hu, *Catal. Lett.* 84 (2002) 107–113.
- [20] J. Cinibulk, Z. Vít, *Appl. Catal. A* 180 (1999) 15–23.
- [21] J.R. Anderson, K.C. Pratt, *Introduction to Characterization and Testing of Catalysts*, Academic Press (Harcourt Brace Jovanovich, Publishers), New York, 1985, p. 64.
- [22] Z. Vít, D. Gulková, L. Kaluža, M. Zdražil, *J. Catal.* 232 (2005) 447–455.
- [23] T. Klicpera, M. Zdražil, *J. Catal.* 206 (2002) 314–320.
- [24] J. Ren, A. Wang, X. Li, Y. Chen, H. Liu, Y. Hu, *Appl. Catal. A* 344 (2008) 175–182.
- [25] V. Sebastian, S. Irusta, R. Mallada, J. Santamaría, *Catal. Today* 147S (2009) S10–S16.
- [26] V. González-Peña, I. Díaz, C. Márquez-Alvarez, E. Sastre, J. Pérez-Pariente, *Micropor. Mesopor. Mater.* 44–45 (2001) 203–210.
- [27] R. Luque, J.M. Campelo, D. Luna, J.M. Marinas, A.A. Romero, *Micropor. Mesopor. Mater.* 84 (2005) 11–20.
- [28] G. Crépeau, V. Montouillout, A. Vimont, L. Mariey, T. Cseri, F. Maugé, *J. Phys. Chem. B* 110 (2006) 15172–15185.
- [29] A. Corma, B.W. Wojciechowski, *Catal. Rev. Sci. Eng.* 24 (1982) 1–65.
- [30] F.M. Bautista, J.M. Campelo, A. García, D. Luna, J.M. Marinas, A.A. Romero, *Catal. Lett.* 24 (1994) 293–301.
- [31] T.Ch. Tsai, S.Y. Chang, I. Wang, *Ind. Eng. Chem. Res.* 42 (2003) 6053–6058.
- [32] N. Satoh, J.-i. Hayashi, H. Hattori, *Appl. Catal. A* 202 (2000) 207–213.
- [33] W.A. Spieker, J.R. Regalbuto, *Chem. Eng. Sci.* 56 (2001) 3491–3504.
- [34] J.T. Miller, M. Schreier, A.J. Kropf, J.R. Regalbuto, *J. Catal.* 225 (2004) 203–212.
- [35] R. Contreras, R. Cuevas-García, J. Ramírez, L. Ruiz-Azuara, A. Gutiérrez-Alejandre, I. Puentel-Lee, P. Castillo-Villalón, C. Salcedo-Luna, *Catal. Today* 130 (2008) 320–326.
- [36] Z.R. Ismagilov, S.A. Yashnik, A.N. Startsev, A.I. Boronin, A.I. Stadnichenko, V.V. Kriventsov, S. Kasztelan, D. Guillaume, M. Makkee, J.A. Moulijn, *Catal. Today* 144 (2009) 235–250.
- [37] J. Leglise, J.N.M. van Gestel, L. Finot, J.C. Duchet, J.L. Dubois, *Catal. Today* 45 (1998) 347–352.